We are IntechOpen,
the world's leading publisher of
Open Access books
Built by scientists, for scientists

4,800
Open access books available

122,000
International authors and editors

135M
Downloads

Our authors are among the

154
Countries delivered to

TOP 1%
most cited scientists

12.2%
Contributors from top 500 universities

CLARIVATE ANALYTICS
BOOK CITATION INDEX
INDEXED

WEB OF SCIENCE™

Selection of our books indexed in the Book Citation Index
in Web of Science™ Core Collection (BKCI)

Interested in publishing with us?
Contact book.department@intechopen.com

Numbers displayed above are based on latest data collected.
For more information visit www.intechopen.com

Osteocytes Characterization Using Synchrotron Radiation CT and Finite Element Analysis

Zully Ritter[1], Andreas Staude[2], Steffen Prohaska[3] and Dieter Felsenberg[1]
[1]Charité Universitätsmedizin Berlin
[2]Federal Institute for Materials Research and Testing, BAM
[3]Zuse Institute Berlin, ZIB
Germany

1. Introduction

Since a correlation between osteocyte number and their morphology with bone aging or its response to pharmacological treatment appears to exist, a methodology to characterize osteocytes from bone biopsies becomes important. In this chapter, the usage of synchrotron measurements, algorithms for image analysis (Amira, ZIB), and the finite element method using parallelized computational resources for topological analysis of osteocytes is explained and discussed. Different routines normally applied for material characterization of network-like structures (skeletonization) have been adapted to visualize osteocytes along bone cement lines at high resolution (2.174 μm). The different steps concerning to counting osteocytes and analyzing the mechanical behavior of bones are illustrated with an example.

The methods were developed to answer some scientific questions such as: Does bone osteocyte distribution, number and volume differ between healthy and osteoporotic bone? How much does the osteocytes' morphology and topology contribute to load transmission capacity in bones? Which parameters are useful to characterize bones and their changes due to aging? Which strategies can be used to maintain a balance of osteocyte number and connectivity in order to balance for minimizing bone aging effects?

Usage of the combined methodologies from CT up to numerical analysis (fem) are presented in this chapter in an easy, feasible and repeatable way allowing osteocytes characterization, whose topology is an indicator of bone adaption under different mechanical or pharmacological conditions. The interdisciplinary work between Charité Universitätsmedizin Berlin (Center for Muscle and Bone Research), BAM (federal Institute for Materials Research and Testing) and Zuse Institute Berlin (ZIB) was essential for quantifying and characterizing osteocytes at different age stages. The required techniques, advantages and disadvantages of the combined methods as well as the expected results are discussed in the chapter.

1.1 Scientific background

Osteocytes are differentiated bone cells from osteoblasts, which are embedded into osteons and connected in between by means of their processes. There is evidence that osteocytes are

not only responsible for sensing mechanical stimuli but also for transmitting the amplified signal to the bone surface (You *et al.* 2001; Cowin 2002; Whitfield 2003; Han *et al.* 2004; Anderson *et al.* 2008; Jacobs *et al.* 2010; Cheung *et al.* 2011). In normal conditions, the sensed mechanical stimulus is transduced in biochemical and bioelectrical signals captured for the osteoblast and osteoclast thus starting bone formation and bone resorption activities. At a macro level, the bone geometry and density is continuously adapted to guarantee bone mechanical functionality under physiological loads. It is known that bone adaption follows the Wolf's and Roux's rules for allowing maximal strength by optimized bone mass.

A misbalance in this process (osteocytes-mechanosignal transmission-osteoblastic and osteoclastic activities) will generate changes in the bone geometry and density distribution such as observed in bone diseases. In the elderly, a misbalance between an accelerated osteoclastic activity and an incapacity of osteoblasts to form new bone results in a progressive reduction of the trabecular bone structures, an increment in the cortical porosity and a reduction of the cortical thickness. At a micro-level, bone is a composite material formed by hydroxylapatite and collagen. Other alterations in the signal pathway from osteocytes to osteoblasts and/or osteoclasts are related with induced changes in the hydroxylapatite crystals by increased secretion of Ca. Thereby the hydroxylapatite crystal number increases and the collagen content decrease and a glass-like bone structure is formed (osteogenesis imperfecta) (Boyde *et al.* 1999; Roschger *et al.* 2008; Dong *et al.* 2010). Similarly, an overproduction of collagen fibrils results in a hyper elastic bone material with a gummy-like mechanical behavior (osteomalacia) (Feng *et al.* 2006). In all cases, osteocytes generated signals appear to be associated with these bone diseases. Osteoporosis is one of the most frequent bone diseases affecting the elderly population, whose number will probably sharply increase in the future, thus we will concentrate firstly in the analysis and comparison of osteocytes from osteoporotic in comparison with healthy bone biopsies. The method explained here is of course applicable independently of the bone biopsies or disease type, including bone samples after pharmacological interventions.

As the signal coming from the osteocytes will stimulate both bone formation and bone resorption, many pharmacological interventions try to effect the receptors for these signals: osteoblast and osteoclast, more than acting directly on the osteocytes. Additionally, it is known that bone resorption velocities are in general higher as required for bone formation (Huiskes 2000; Liu 2001; Nabavi *et al.* 2001; Huang *et al.* 2010). The pharmacy industry develops therefore principally antiresorptive drugs, which will reduce or inhibit osteoclastogenesis. The most used antiresorptive drugs are bisphosphonates, estrogen receptor modulators (SERMs), calcitonin, parathyroid hormone (PTH), cathepsin K inhibitors, Denosumab and strontium ranelate. This last drug might not only have an antiresorptive effect but is also able to stimulate osteoblastic activities. However, it is not clear how much the hydroxylapatite crystal is morphologically changed by replacement of Ca atoms through Sr atoms. Thus it is unclear how much the densitometric measurements are affected. Osteocytes characterization from bone biopsies of patient treated with strontium ranelate will help to illustrate how osteocytes (and consequently osteoblastic and osteoclastic activities) are affected after alteration of the hydroxylapatite bone crystal.

Bone adaption or its pathological changes in time are nowadays monitored by densitometric and *in vivo* CT or similar radiological measurements. After measurement evaluation, the density bone distribution is calculated by comparison of measured absorptiometry

coefficients with those from phantom measurements of materials of known density values. Cortical bone density and trabecular bone density can thus be determined. After segmentation structural bone parameters such as BV/TV and cortical thickness are calculated. There are additional structural and geometrical parameters (e.g. trabecular thickness, trabecular separation, cortical porosity) that are derived from mathematical relations of the density parameters combined with the geometrical contours or bone segmentation.

Osteoporosis implies a fracture risk whose asymptomatic development is not seriously considered by the affected population. CT-techniques allow analysis of bone structure, geometry and density in time (*in vivo*) or its detailed analysis in nanometer scales by analysis of *in vitro* CT measurements. Actually clinical CTs possess a resolution of 150 µm.

Some indicators calculated after reconstruction and evaluation of bones are widely accepted to show bone adaption and to estimate its fracture risk. Such parameters are however normally given as a mean value over the measured volume. Although these parameters are a good indicator of bone morphology, in some cases they are insufficient to show how bone is responding under a pharmacological treatment or newly adapted conditions. Osteocytes are not only directly responsible for starting bone remodeling regions, but their number, sizes and distribution in comparable bone volumes shows how bone has changed by a disease or by medication that alter bone mineralization such as strontium ranelate or bisphosphonates. We have concentrated on developing a methodology for osteocytes characterization using available commercial platforms and adapted algorithms. Radiological and tridimensional visualization allows understanding how a pathological condition or an alteration of the normal bone conditions is related to the osteocytes morphology and their distribution.

2. Related work

Evidences of osteocytes (monkeys) ultrastructural changes under microgravity (Rodionova *et al.* 2002)

Tensile strains regulate stem cell osteogenesis (Kearney *et al.* 2010)

Maintenance of subject specific cell mechanosensitivity for prevention of osteoporosis (Mulvihill *et al.* 2008)

Osteon diameter is related with the strain environment distribution (van Oers *et al.* 2008)

Osteocytes apoptosis induce angiogenesis (Cheung *et al.* 2011)

Osteonal geometry reconstruction and BMU activity analysis by using SR-CT (osteocytes are aligned around osteon cavities) (Cooper *et al.* 2011)

Specific location of osteon type structures correlate with its mechanical environment (external loads) (Beraudi *et al.* 2010)

It appears that osteocytes are physiologically adapted to "sense" its mechanical environment by means of its primary cilium (Whitfield 2003)

Visualizing osteocytes canaliculi network (limited VOI) able to show 2 osteocytes (lacunae) (Schneider *et al.* 2011)

It appears that osteocytes networks mimic the orientation of the surrounding extracellular bone matrix(Kerschnitzki *et al.* 2011)

3. Methodology

Osteocytes characterization has been made possible by combining radiological, image and numerical analysis. We have employed: laboratory micro-CT and Synchrotron radiation CT (SR-CT) (Rack *et al.* 2008) for radiological *in vitro* measurements, Amira (ZIB) (Stalling 2005) for image analysis and the finite element method (Abaqus) for estimating and comparing compressive stiffness from healthy and osteoporotic bone biopsies after SR-CT measurements. Additional algorithms were implemented in Matlab. Before describing the method in detail general considerations for sample preparation will be discussed.

3.1 General considerations

The first step is the bone sample preparation. Bone samples are normally fixed in methyl methacrylate or in ethanol for tissue conservation. In our study, the biopsies were maintained fixed in 70% ethanol and 30% water for allowing posterior histological analysis (e.g. von Kossa staining) when required. If subsequent analyses are not planned, biopsies embedded in methyl methacrylate guarantee CT measurements free from movement artifacts. Some studies have shown that derived bone structural analysis from biopsies first fixed in ethanol with those after methyl methacrylate do not present significant differences (Perilli *et al.* 2007). An ethanol fixation allows adapting the container to the requirements of the CT acquisition. In case of using an ethanol fixation, the samples should be acclimated to the ambient room temperature previous to SR-CT measurements, in order to avoid micro-movements during the measurement.

The method from CT measurement up to FE Analysis includes the following steps:

Task 1:   Bone biopsies extraction
Task 2:   Laboratory µCT measurements *in vitro* (minimal resolution: 20 µm)
Task 3:   3D projections reconstruction
Task 4:   Standard bone structure and density parameters calculation (e.g. BT/TV, Trabecular Number (Tb.N), Trabecular Separation (Tb.Sp))
Task 5:   Selecting bone biopsies for SR-CT (based on compared parameters in task 5 (e.g. samples with a BV/TV variation > 60%)
Task 6:   Preparation of tailored bone containers for SR-CT measurements
Task 7:   Repeating Task 3 to Task 5
Task 8:   Image analysis including 3D stereoscopy (Amira)
Task 9:   Analysis of osteocytes topology (number and volume) by adapting skeletonization techniques
Task 10: Comparison of obtained results in Task 9
Task 11: Finite element mesh generation (script in Matlab interface Amira-Abaqus (for Amira version previous to 2010)
Task 12: FEA and generation of comparative histograms from mechanical parameters (von Mises, minimum principal strains)
Task 13: Comparison of obtained results in Task 12

3.2 Detailed methodology description

3.2.1 Task 1: Bone biopsies extraction

In our example study an analysis of the jaw was performed. For comparison and results interpretation, the regions of interest selected for study need to be biomechanically comparable. In our case, bone samples were extracted from region 36. For analysis of osteocytes morphological changes after prostheses implantation, it is recommendable not only to compare biopsies from the same regions of healthy subjects but with biopsies taken from the contralateral bone side of the same subject. The implantation of prostheses implies drastic induced changes in the mechanical bone environment, thus significant differences on osteocytes morphology could be erroneously measured by comparing with healthy subjects. On the other hand, considering that bone biopsies are an invasive procedure, an alternative would be to extract the biopsies at least one year after implantation, time in which bone adaption velocity achieves normal balanced levels again. After extraction, bone samples were maintained under routinely used conditions of constant -20°C temperature.

Since osteocytes characterization is basically performed by means of SR-CT measurements, a highly specialized technique, it is recommendable to pre-select the best biopsies that could show typical patterns for the bone disease or bone topic under study. We recommend, therefore, a previous image analysis using a typical CT laboratory such as outlined in task 2.

3.2.2 Task 2: Laboratory µCT measurements *in vitro* (minimal resolution: 20 µm)

SR-CT is a specialized CT measurement, which is time consuming and requires knowledge and good planning. Therefore, to obtain better results, the regions to be analyzed with this technique need to be firstly pre-selected after analysis and comparison of the bone structure and density parameters coming from, for example, laboratory CT measurements. In most of the cases, biopsies have typical dimensions of 2 mm in diameter and 10 mm in length. Cone-beam CTs with a resolution between 15 and 20 µm will be sufficient to determine bone structure and density. A high-energy X-Ray source will allow good contrast and reduced noise, thus improving measurement quality. For our study, we used 20 µm and a cone beam CT using 100 kV and 30 µAmpere. Flat and dark exposures were taken before and after the measurement, averaged, and used for correcting the projections.

3.2.3 Task 3: 3D reconstructions

After projection filtering, maximal and minimal values of the gray values corresponding to the attenuation coefficients of the bone are obtained. In general it is not recommendable to perform additional Gauss filtering to reduce the noise. This will results in loosing important information concerning the bone trabecular structure. Instead, a good segmentation is preferred. Analysis of the histograms of the gray value distribution from in the best case a random selection including 50% of the samples from each group or at least one sample from each group under study (here osteoporotic vs. healthy bone) allows the determination of the threshold values required for segmentation. The valleys formed between each peak-value in the histograms indicate the appropriate threshold values to be used. Advanced image analysis software such as Amira (ZIB) possesses tools (e.g. magic wand) for improving the segmented bone/material regions. This threshold needs to remain constant until finalizing the study, since calculation of bone structure, geometrical and density parameters depend on it. The BV/TV is the most accurately determinable structure parameter. Using the contours at the

perimeter in each transversal segmented projection and filling the total area inside, the total volume containing the biopsy will be determined (BV). After determination of the bone volume from the segmented region, the tissue volume (TV) value will be determined. Thus the BV/TV ratio can be calculated. Once the BV/TV has been calculated for all biopsy samples and after comparison between the groups under study, it is recommendable to select biopsies with a difference larger than 60% in the BV/TV ratio between groups (here healthy vs. osteoporotic bone biopsies from the same jaw region (e.g. for our sample 36).

In a similar way as described above, 3D segmentation after SR-CT measurements can be performed.

3.2.4 Task 4: Standard bone structure and density parameters calculation (e.g. BT/TV, Trabecular Number (Tb.N), Trabecular Separation (Tb.Sp))

Commercial CTs scanners are able to perform an automatic evaluation of BV/TV and other structural and geometrical parameters. The most relevant structural bone parameters are Tb.N, Tb.Sp, cortical thickness (Ct.Th.), cortical perimeter (Ct.Pt), and from the density parameters group, cortical (Dcomp) and trabecular density (Dtrab). Frequently other parameters are reported (e.g. density at the center of the bone section: Dmeta, or immediately near to the cortical bone (Dinn) but these are mathematically derived from the Dcomp und Dtrab in combination with their geometrical location. In similar form, series of structural parameters can be mathematically obtained from BV/TV in combination with superimposed geometrical forms (e.g. spheres or ellipses). A linear relation of the measured attenuation coefficient distribution to the bone volume allows assignment of density values for each voxel.

3.2.5 Task 5: Selecting bone biopsies for SR-CT (based on compared parameters in task 5 (e.g. samples with a BV/TV variation > 60%)

As explained above, the BV/TV ratio is easy to calculate, without employment of external software. A non-automatic calculation allows following the process and to improve segmentation if required. The BV/TV will be calculated from standard laboratory CT-measurements (at least 20 μm). After that and for synchrotron radiation measurements, specimens with a difference of 60% in the BV/TV value between groups (e.g. osteoporotic vs. healthy) will be chosen for osteocytes morphology characterization.

3.2.6 Task 6: Preparation of tailored bone containers for SR-CT measurements

Containers with dimensions as close as possible to the biopsy dimension need to be selected. In our study, the containers were tailored +10% of the biopsy diameter. At such scales, it is recommendable first to fill the container partially with the ethanol solution (if applicable) to avoid air bubbles formation under the biopsy, to introduce the bone sample, and to continue up to complete filling. High temperature variations need to be avoided for suppressing possible additional movement artifacts.

3.2.7 Task 7: Repeating Task 3 to Task 5 (from SR-CT-measurements up to 3D volume reconstruction)

For SR-CT measurements with a pixel size of 2.174 μm of the total biopsy (height ca. 1 cm), two stacks each one with 2500 slices are required. Due to the high variability of the beam, flat exposures are collected every 100 projections.

For each data set the rotational axis can numerically determined. From this, the tilt angle and displacement are calculated for eliminating double contours, also allowing correction of each slice separately. An important aspect is to control the existence of ring artifacts, which in the case of our data is mainly caused by damages of and pollutions of the scintillator. If the location of the defect region is known, the attenuation coefficient corresponding to the region can be averaged from the neighbors and corrected computationally during the reconstruction process. The flatfield corrected projection data are filtered with a 3x3 median filter and reconstructed using a standard filtered back-projection algorithm with only a ramp filter. Thus the spatial resolution is degraded less than when using a smoothing filter (e.g. Shepp-Logan) and the high frequency noise is suppressed sufficiently.

3.2.8 Task 8: Image analysis including 3D stereoscopy

After segmentation and assignment of gray value ranges to each specific material, here bone and osteocytes, the first characterization parameter related to osteocytes characterization, that is their localization, will be obtained. For analysis of osteocytes trajectories, it is highly recommendable to use 3D stereoscopic views of the generated osteocyte surfaces embedded on the bone tissue. 3D-stereoscopy allows a detailed description of the trajectory especially in the trabecular bone volumes, in which the classical circular lamellae around the osteons are not visualized. By superposition of the orthoslices and using a minor contrast canal on the reconstructed volume, the osteocytes trajectories and patterns can clearly be identified; in this form, their relation to the cement lines location becomes understandable.

3.2.9 Task 9 - 10: Analysis of osteocytes topology (number and volume) by adapting skeletonization techniques

Once the projections from the SR-CT measurements containing the gray values have been reconstructed for each stack, this will be positioned and merged to obtain the total CT-biopsy measurement. A review of the orthoslices can be made for checking ring artifacts. For segmentation in Amira, a "label voxel" tool can be used for supplying the limit threshold values of the gray scales to separate each material type, or grade of mineralization in the bone label. In our study, the different grades of mineralization on the bone volume were not segmented separately. Air/Exterior, bone, osteons and osteocytes were segmented. As osteons canals, osteocytes (lacunae) and the exterior/air regions will have similar attenuation coefficients, making it difficult to determine an appropriate threshold value for osteocytes segmentation, it will be simple and semiautomatic to enable the options "voxel accuracy" and "bubbles" in Amira (ZIB) using the "label-voxel" toolbox. Thus the osteons will be segmented (separated using the magic wand). This tool causes all connected voxels with same material properties to be selected, separating osteons from osteocytes. The remaining bubble voxels could be adjudicated to "osteocyte" material. Optimal results depend on the grade of contrast and reduced noise of the original CT measurement. As mentioned above, at this scale, it is not recommendable to use Gauss filters or similar. Instead a good segmentation could be used. After segmentation, the number of the voxels for each material region (bone, osteons and osteocytes) and its total volume is determined (material statistics in Amira). Thus the relations total volume (biopsy volume)/tissue (bone) volume and total volume (bone)/tissue (osteocytes) volume are determinate.

Osteocytes number calculation. The osteocytes number can be calculated after skeletonization (Fouard *et al.* 2006) of the segmented biopsy, in which only the osteocytes

are kept. Thus, the other materials should be selected and deleted only for this step (of course after saving the original Amira mesh containing all material regions). A skeleton is a schematic representation of a solid after extraction of geometrical and topological simplified shape features, thus facilitating its analysis on the extracted schema. In biomechanics this tool is commonly used for analysis of the nerve or the circular systems (e.g. diameter and length distribution of the vessel is obtained). The distant transformation map concept introduced by H. Blum calculates the closest boundary (vertices) for each point in the represented object. In the case of the osteocytes, this results in a center point inside the surface (bubble) at each osteocyte (Fig. 9). For large osteocytes, a two vertices joined by one line will be generated. Looking at the skeletonization results, the total number of vertices and lines corresponding to the segmented osteocytes are reported. The osteocytes number (N) is calculated subtracting the number of vertices (v) from the number of lines (l). This simple method was tested and validated by automatic counting compared with a manual counting of osteocytes in a reduce volume of the biopsy.

3.2.10 Task 11: Finite element mesh generation

After segmentation and previous to osteocytes counting procedure, a surface for each material is obtained. For mesh generation the semi-automatic tool from Amira ("tetragen") was employed. The triangular surface is then converted to solid tetrahedrons. Requisite for successful 3D meshing are that the triangulated surface fills the criterions of non-intersection, surface closeness, aspect ratio and non-wrong conserved orientation. Once the surface is ready, the tetrahedral mesh is automatically generated using an advancing front algorithm implemented in Amira. Prior to mesh generation, it is recommendable to check the number of expected finite elements. If the represented geometry is not affected, improvements in the mesh generation could be allowed. Finally, the mesh topology (coordinates and elements connectivity) can be written in an ASCII format, readable for the most common FE solvers (Abaqus, Ansys, etc.).

3.2.11 Task 12: FEA and generation of comparative histograms from mechanical parameters (von Mises, minimum principal strains)

In our study, the mesh topology was imported in Abaqus. Using Abaqus-CAE the boundary conditions, material properties and mechanical material behavior will be imposed in the solid model of the bone volume with the osteocytes. A compression test was simulated by encastring the nodes (all six degrees of freedom = 0) at the basis of the mesh and a distributed load on the top of the model. For comparison with other studies, the material properties were taken from literature (Boutroy *et al.* 2008; Rincon-Kohli *et al.* 2009; Varga *et al.* 2011; Vilayphiou *et al.* 2011). The materials were modeled to be isotropic and homogeneous and to possess a linear elastic behavior. The Abaqus solver was used to calculate the strain and strength tensors. After analysis, reports (ASCII format) containing the magnitude of each mechanical parameter amount others (e.g. minimum principal strains and von Mises stress distribution) were exported for post-processing analysis. The magnitudes were averaged at the centroid of each element. Lists containing the element number and corresponding strength/strain values were represented in histograms in pre-selected thresholds. Logarithms representations of such distributions will conduce to wrong results interpretation. Thus, a natural scale of percental number of elements at each interval is preferred.

3.2.12 Task 13: Comparison of obtained results in Task 12

Traditionally, the power of the finite element analysis is to show zones of high stress or strains concentration, which are indicators of regions susceptible to mechanical failure, thus allowing redesigning by re-dimensioning or improving the strength or mechanical properties of the materials. For the analysis of biological tissues, it is not only important to visualize these zones of high stresses but to compare the effect of pharmacological interventions on the bone or the effect of artificial implants and to quantify these effects on bone tissues even at short times. Histogram distributions of stress and strains in pre-defined thresholds are used for this. Explicitly in the case of osteocytes, the zones of stress concentration were visualized and histograms were elaborated for analysis and comparison of the effect of the size, number and location on bone strength for osteoporotic and healthy biopsies of the jaw. For histograms, interpretation of the translational displacement and the picks of the histograms were analyzed. Translational displacement differences between groups (osteoporotic vs. healthy bone biopsies) are indicator of the compressive bone stiffness. If the histogram curve tends to be localized to the left (Y axis), a high percentage of finite elements possesses low stress values, thus indicating that the bone are more mechanically stable. On the other hand, the differences of the height of the histogram (Gauss distribution) are an indicator of stress concentration, thus under same mechanical boundary conditions, a sample experiencing highest magnitudes of stresses (highest pick) is less able to resist and to transmit external acting physiological loads, which imply highest damage tendency under physiological load (bad mechanical bone quality). The histogram generation and their comparisons can be performed by writing a simple Matlab subroutine or amongst others using the Python programming language.

4. Practical example (results)

Biopsies from osteoporotic and healthy bones were analyzed. The results from each of the task described above will be presented.

4.1 Task 1: Bone biopsies extraction

No special techniques were employed for bone biopsy extraction and no post-traumatic events were registered.

4.2 Task 2 - 6: Laboratory µCT measurements and 3D reconstruction *in vitro*

In an initial step, 20 healthy and 20 osteoporotic bone biopsies were scanned using an isotropic resolution of 20 µm. Three-dimensional volume reconstructions and image analyses performed using Amira (ZIB) are shown in the Fig. 1. A voxel based density distribution color map (red-orange: from low to middle density values and from yellow to white: highest density values) was used to identify new bone from old one, as well as the differently mineralized bone regions. After analysis of the histogram distributions of the gray values obtained from the CT-measurements (segmentation), the BV/TV ratios were calculated using the procedure explained above. Exemplarily, the calculated values are reported at the bottom of the figures 1 and 2. As observed, the highest calculated BV/TV differences were registered for the biopsy fr2 (from the healthy group at the center in Fig. 1) with a BV/TV= 0.3426 and for the biopsy fr7 (from the osteoporotic group at the right in Fig. 2), thus these two biopsies were selected for

SR-CT measurements to find out if the number of osteocytes, their volume, and their distribution along the cement lines are correlated with aging.
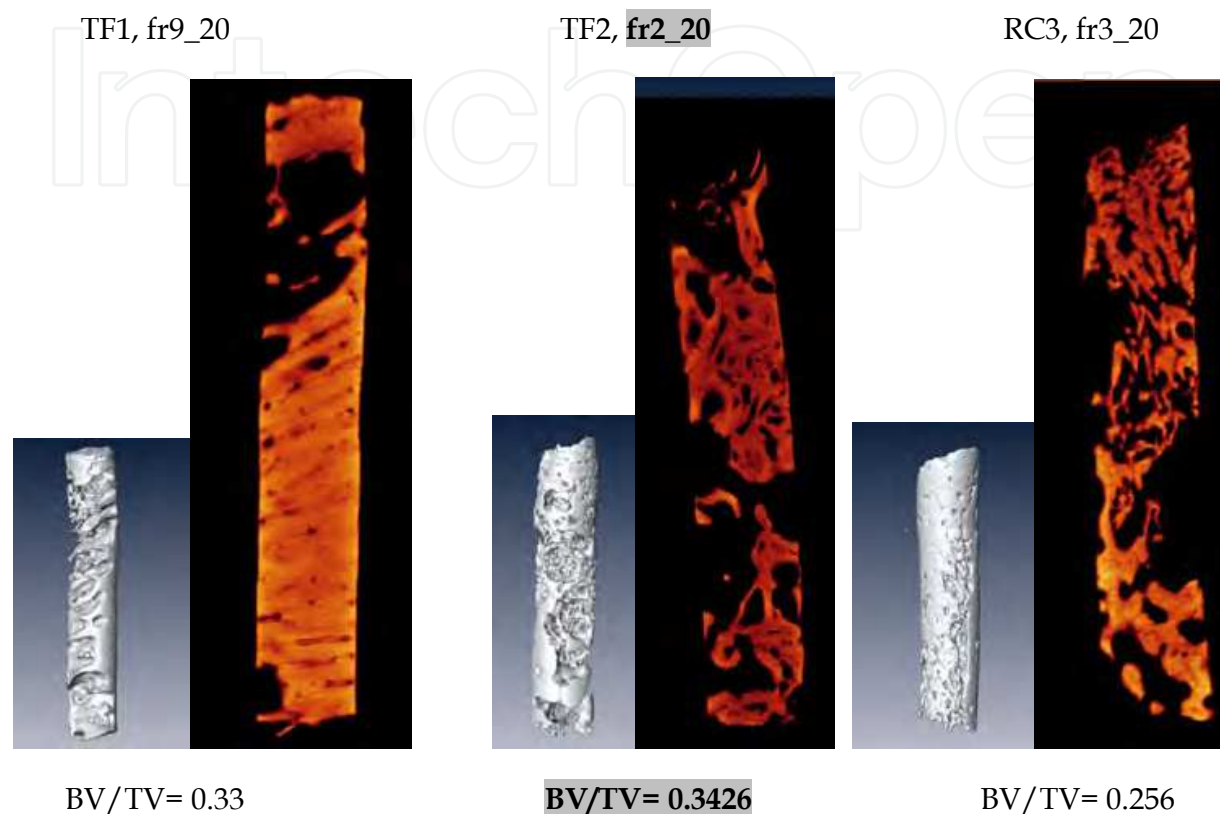
TF1, fr9_20   TF2, **fr2_20**   RC3, fr3_20

    BV/TV= 0.33   **BV/TV= 0.3426**   BV/TV= 0.256

Fig. 1. Healthy bone biopsies from the jaw: 3D reconstructions and BV/TV determination after µCT laboratory measurements (20 µm isotropic resolution).

4.3 Task 8: SR-CT image analysis including 3D stereoscopy

4.3.1 Task 8.1: Image analysis

As explained above, after SR-CT measurements (ca. 5000 slices @2.174 µm isotropic resolution), the volumes were visualized using Amira (ZIB) as shown in the Figure 3. It appears that the osteocytes are more frequent in the healthy biopsy and that they are shorter compared with the osteoporotic one. Outside of osteons the osteocytes are localized along the cement lines. Additionally they seem to be more frequent in the high mineralized regions (more lightening voxels) as shown in the selected axial and orthogonal slices of the Fig. 3. In the Fig. 4, a view of the 3D volume reconstructions (osteoporotic and healthy) and a detail from the osteoporotic bone biopsy (fr7) through a slice using an inverse color map shows that near the bone surface osteocytes are minor in number and the bone appears to be less mineralized. Confirming the initial observations, osteocytes are mainly localized along to the cement lines and are less spaced inside the highly mineralized regions. Osteocytes distribution (red) embedded in the bone matrix for the healthy bone biopsy (section) are shown in the Fig. 5.

BSch-M4, fr4_20   BH5, fr5_20   KG7, **fr7_20**

BV/TV = 0.2203   BV/TV = 0.237   **BT/TV=0.1791**

Fig. 2. Osteoporotic bone biopsies from the jaw: 3D reconstructions and BV/TV determination after μCT laboratory measurements (20 μm isotropic resolution).
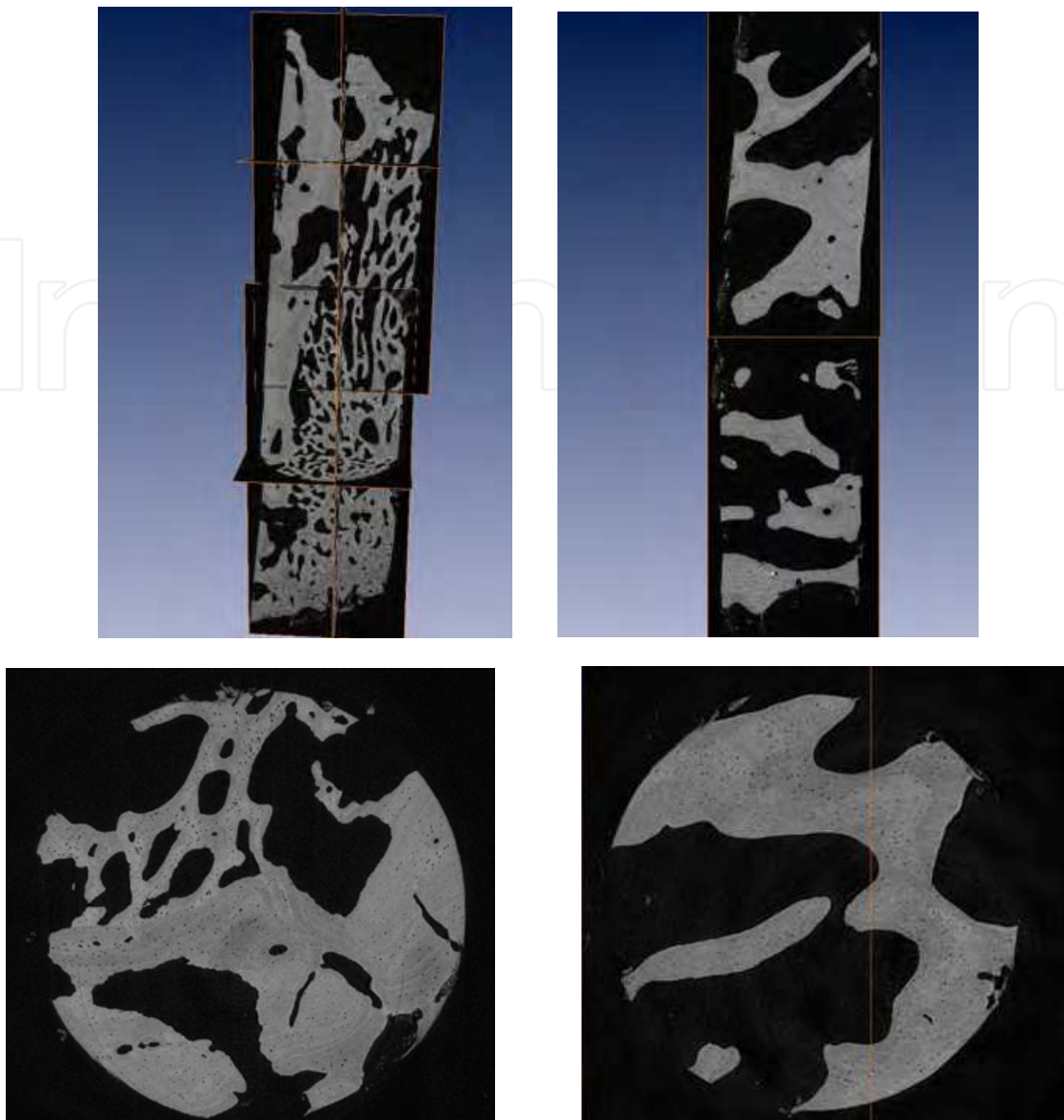
Fig. 3. Axial and orthogonal cuts showing the different grades of mineralization and osteocytes location for a healthy (fr2) and an osteoporotic (fr7) bone biopsy of the jaw region36 after SR-CT measurements @ 2.174 μm (BESSY).

4.3.2 Task 8.2: 3D stereoscopy 🟥 🟦 (Amira ZIB)

Due to the high resolution of the scans, especially for the healthy biopsies in which a large number of osteocytes were visualized, it can be difficult to follow the osteocytes trajectory after surface rendering. We found that using stereoscopic views of the segmented and subsequently rendered volumes of osteocytes facilitates understanding osteocytes morphology. It appears that osteocytes presented an elliptical-like surface and that its major radius is mainly aligned with the longitudinal axis of the biopsies, which represents, in the case of the analyzed regions, the loading axis. Stereoscopic views are essential to understanding how osteocytes are really distributed inside the bone volume (exemplary shown for the osteoporotic bone biopsy; osteocytes colored in yellow (Fig. 6)), and their trajectory is clearly identifiable (Fig. 7).
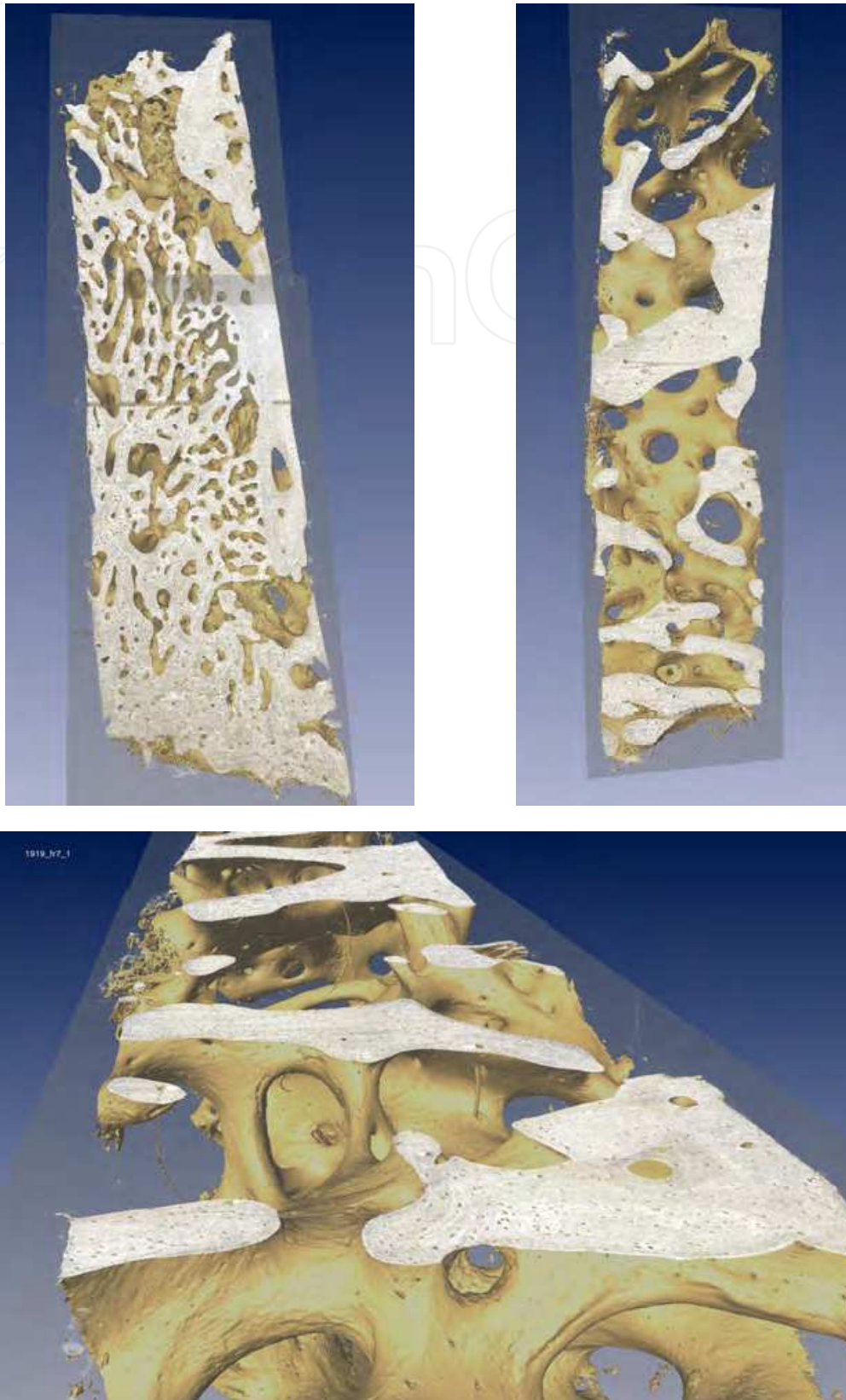
Fig. 4. 3D Reconstruction of a healthy (left) and an osteoporotic (right) bone biopsy after SR-CT measurements (2.174 µm). In slice (inverse color map) different mineralized regions and osteocytes are shown (bottom: detail).
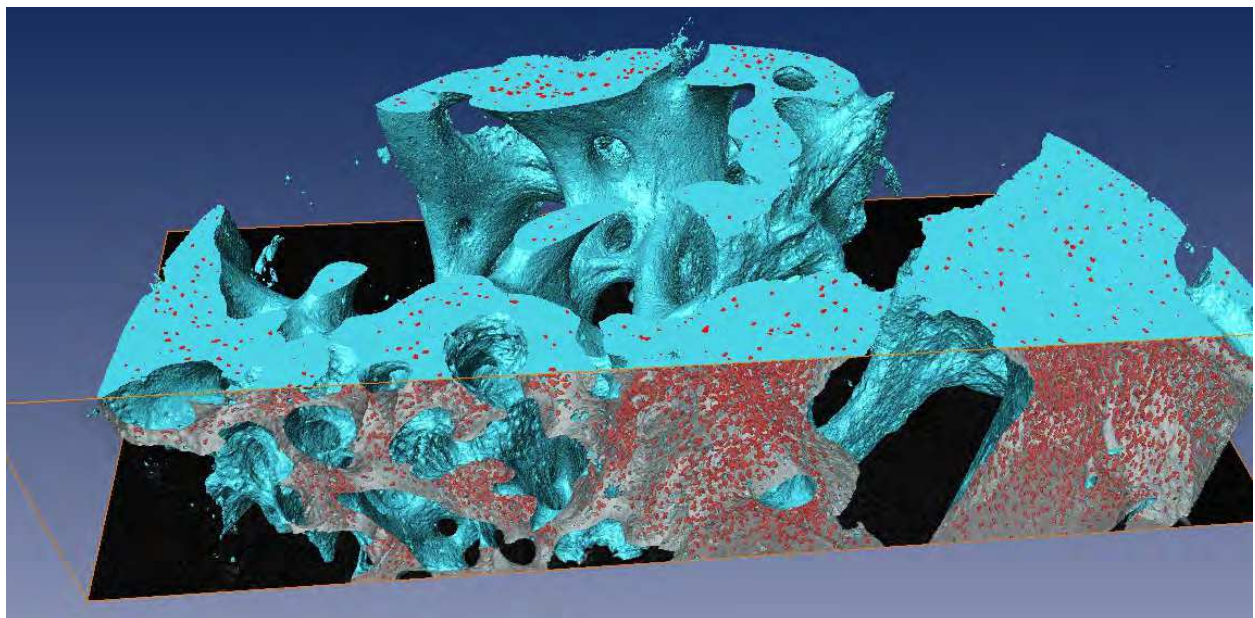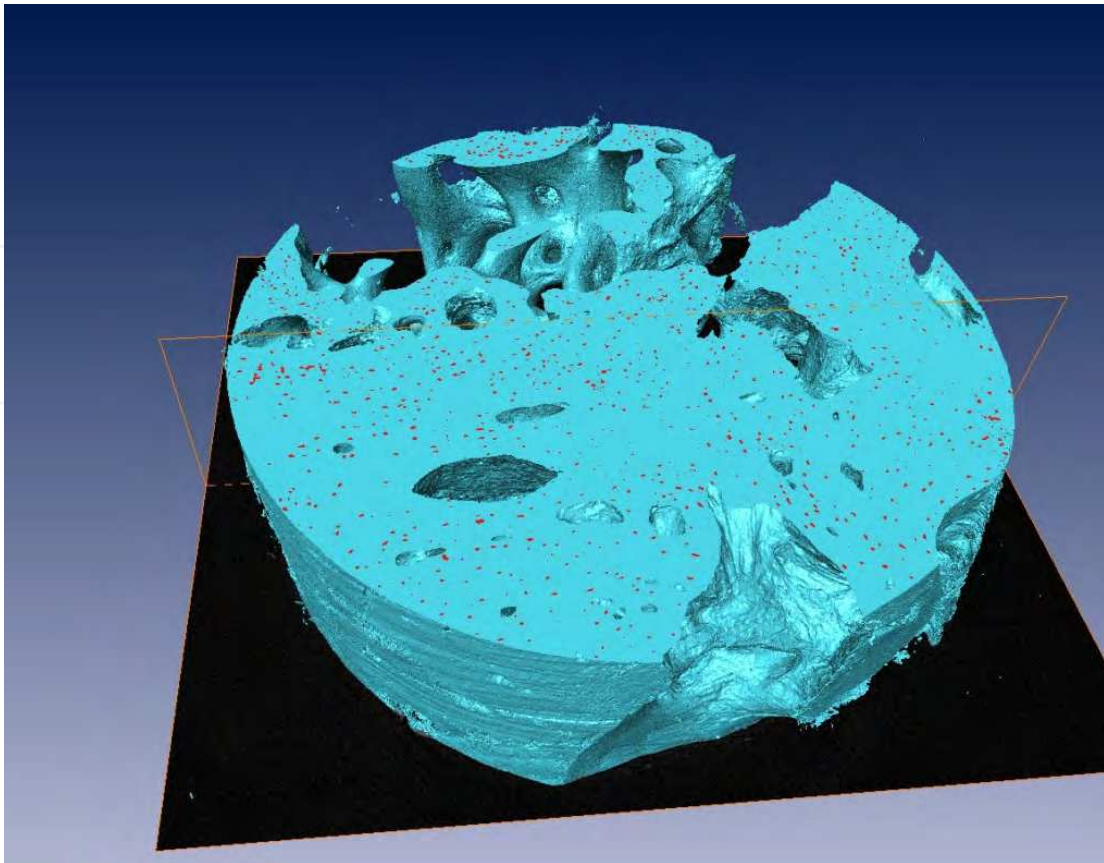
Fig. 5. 3D Volume rendering of a healthy bone biopsy (section) after SR-CT measurements @2.174 µm (BESSY), showing osteocytes (in red) embedded in the bone matrix (Amira ZIB, bottom: cut).

In both samples the osteocytes were localized mainly on the low mineralized regions (qualitatively) or enlarge of the cement lines as show exemplary in a cut of the projections from the healthy bone biopsy (Fig. 8).

The size of the osteocytes was higher in the osteoporotic biopsies. After qualitatively analysis the center points representing each osteocyte were quantified and compared as show in the next section.
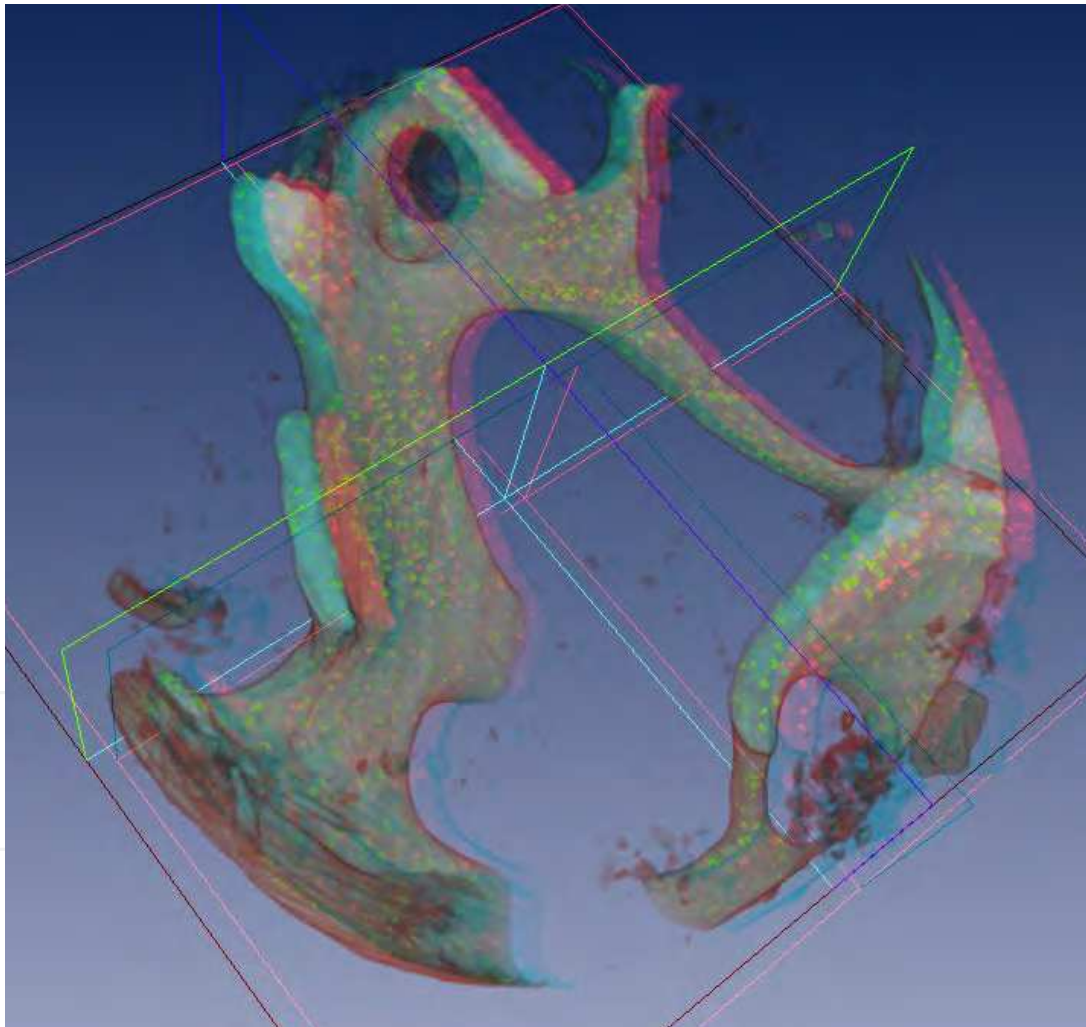
Fig. 6. Example of a stereoscopic 3D view for the osteoporotic biopsy section showing the osteocytes in yellow aligned in the load direction.
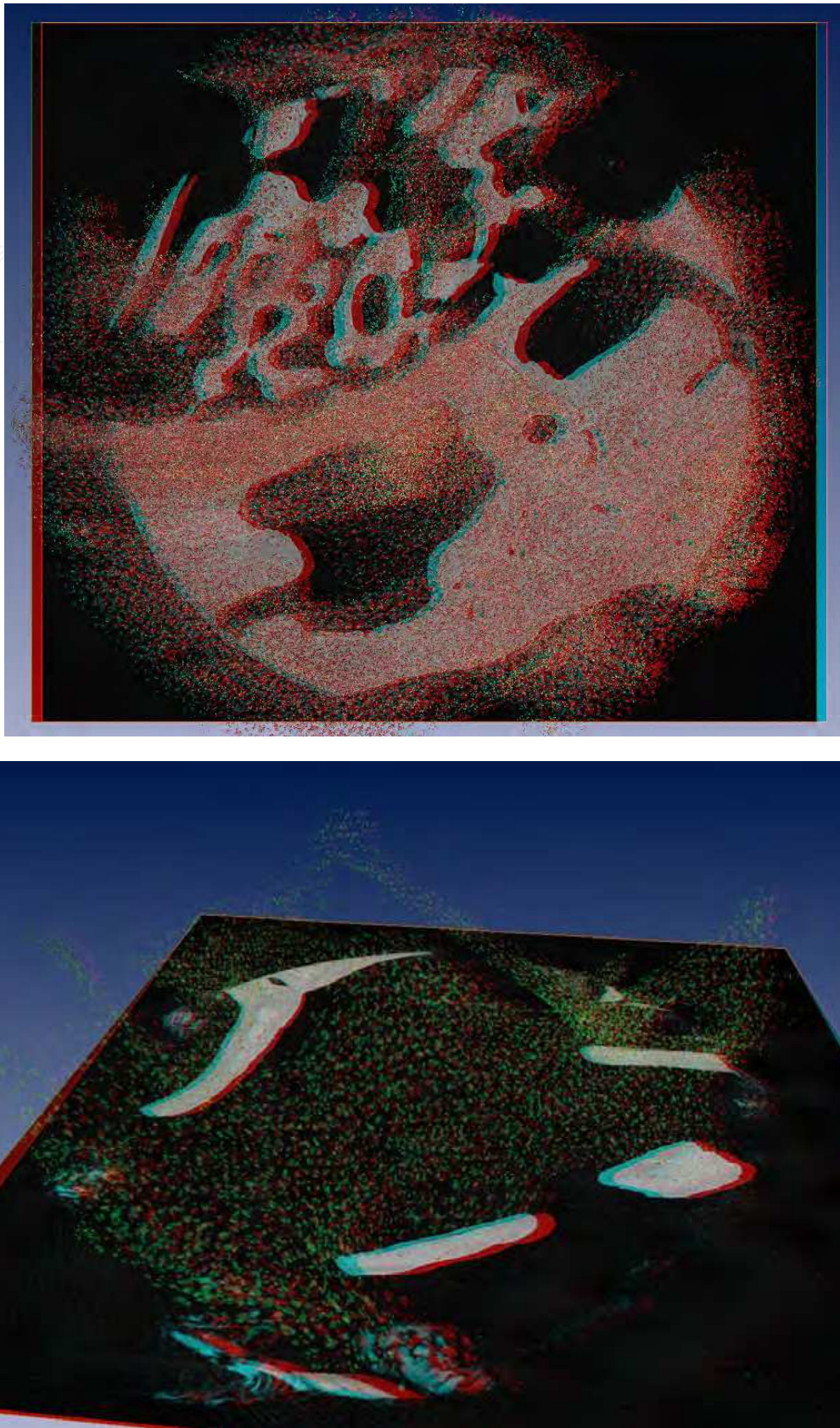
Fig. 7. Stereoscopic view of osteocytes path distribution in a healthy (top) and an osteoporotic (bottom) bone biopsy section.
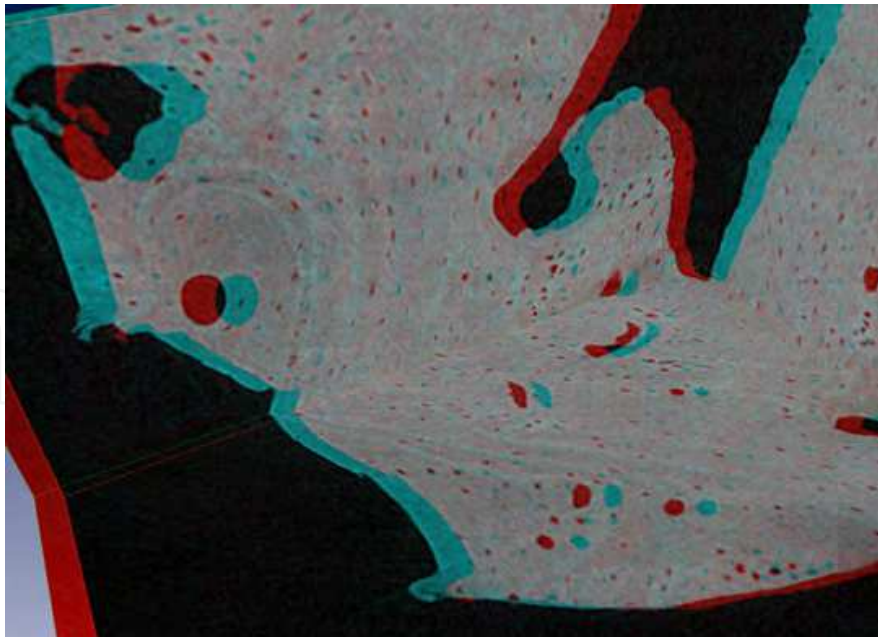
Fig. 8. Stereoscopic view of the projection from the healthy bone biopsy showing the osteocytes aligned along to the cement lines (SR-CT measurements @2.174 μm).

4.4 Task 9 - 10: Analysis of osteocytes topology

After using the skeletonization tool from the voxel topology as described in 4.2.9, the osteocyte number was determined, which was larger in a healthy bone biopsy. To confirm these findings two additional biopsies from the jaw with identical regions, one from an osteoporotic and one from a healthy bone, were analyzed following the same protocol. After comparing osteocytes number quantification (Fig. 10), it was found that osteoporotic bone could have up to of 85.4% (mean comparisons) less osteocytes in the jaw in the same region (36). As healthy bone possesses higher bone mass, the osteocytes number related to the analyzed bone volume (identical biopsy section) as well as the osteocytes volume related to the bone volume were additionally quantified, compared, and shown in Figs. 11 and 12 respectively.
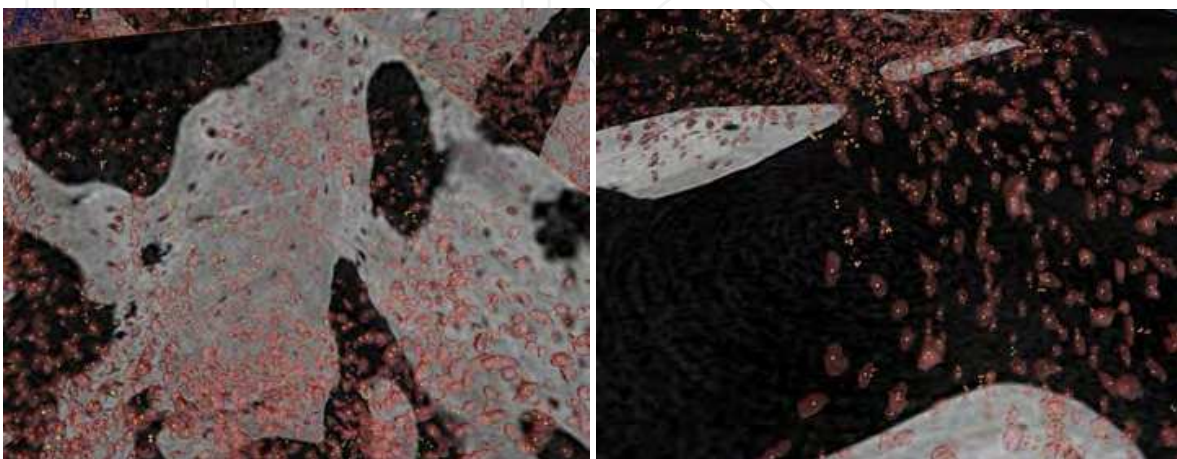
Fig. 9. Osteocytes numbers is calculated by counting the center points inside of each osteocyte surface. Right: osteoporotic and left: healthy bone sample.
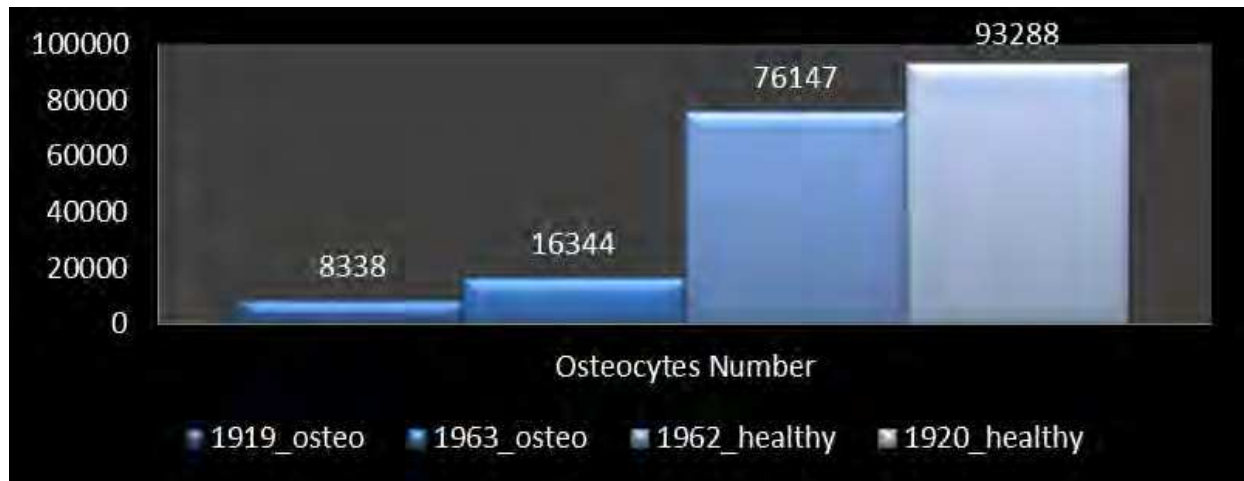
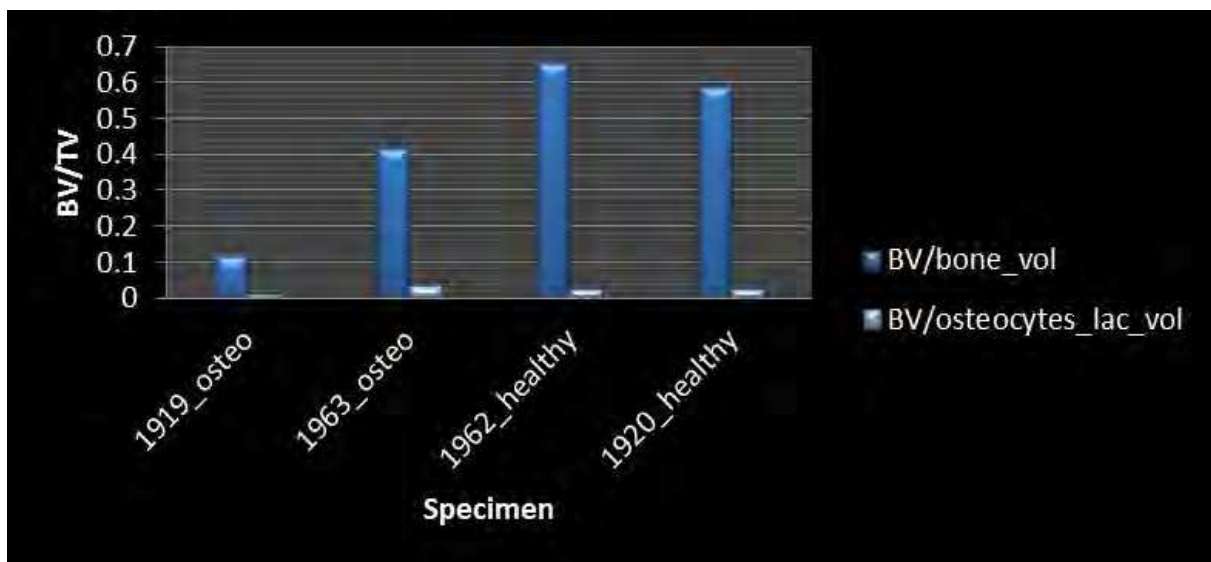Fig. 10. Osteocytes number for healthy and osteoporotic bone biopsies of the jaw (section).
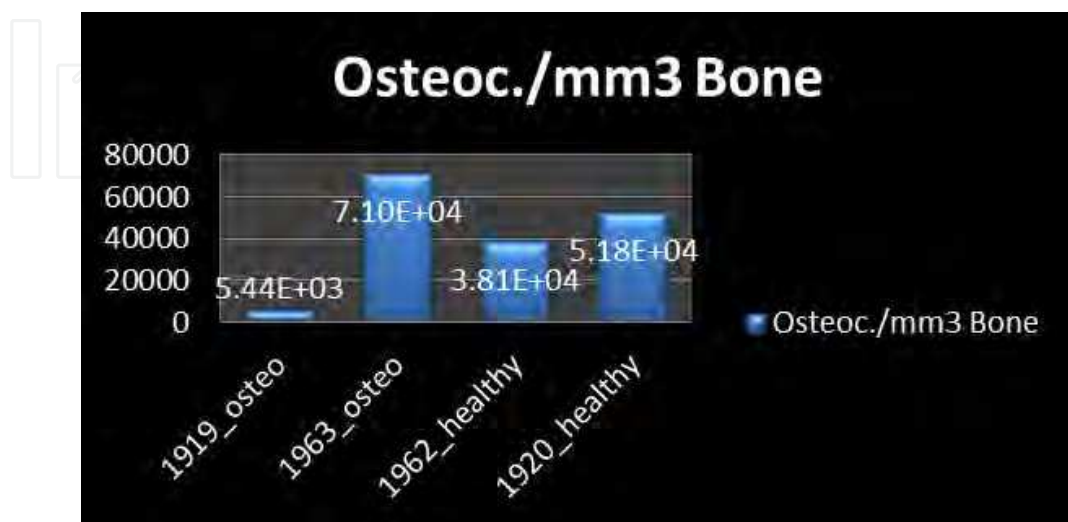

Fig. 11. BV/TV relations.

Fig. 12. Osteocytes number related to the bone volume.

4.5 Task 11 - 13: Finite element analysis

Due to the high computational costs, only a section from the healthy and bone biopsies from equivalent anatomical regions were analyzed. After meshing following the protocol described in 4.2.10, boundary conditions and material properties were imposed in the FE models (Fig. 13 and 14).
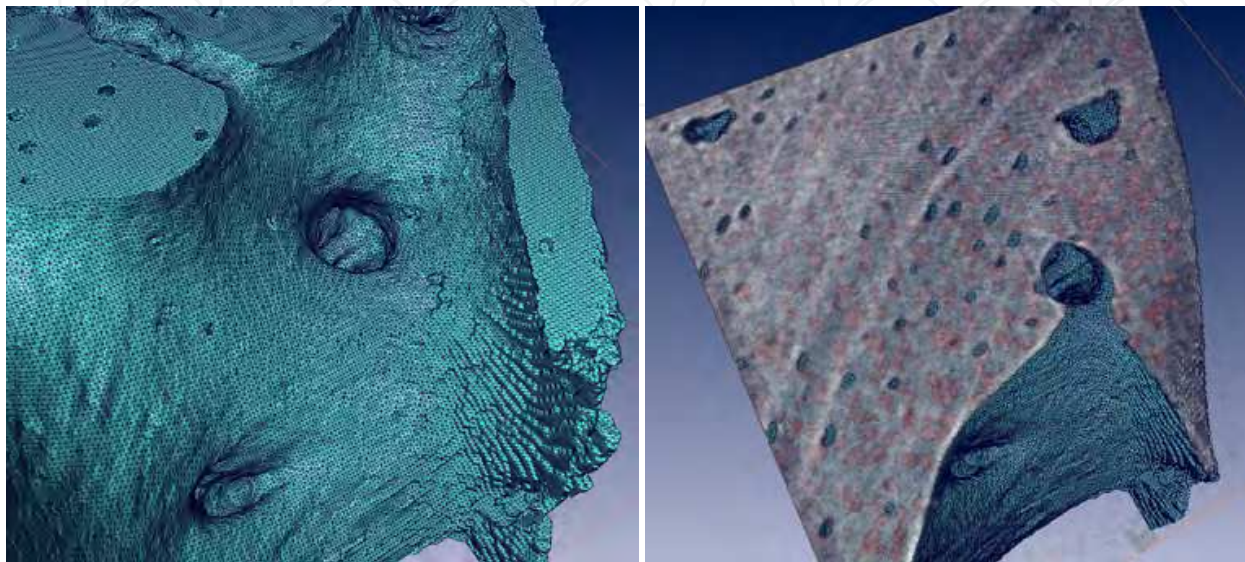

Fig. 13. FEM from a bone biopsy (left) and a zoomed section (right) with a cutting plane showing the projection in a false color map and the meshed osteocytes inside in red.

For osteocytes an elastic Young modulus of 1% of the elastic modulus of bone was given. Due to the fact that with the used resolution it was not possible to visualize the canaliculi, non-hydrostatic properties were chosen for the osteocytes. Thus for the same reason and in order to keep simplicity, the bone was not modeled as biphasic but as homogenous, isotropic and linear elastic. To compare with other studies, in which *in vivo* analysis of human μFE-models has been analyzed, material properties and boundary conditions (load magnitude and application) were taken from literature. Thus, an E-modulus of 17 GPa, a Poisson ratio (γ) of 0.3 and 1.7 GPa and γ = 0.45 for bone and osteocytes were used respectively. As explained above the differently mineralized regions were not segmented and consequently meshed together. Similarly for comparison with other analyses, a compression load of 1000 N was applied ramp-like and linear in the step. The step has a total time of 100 seconds, and reports of the results were set to be printed each 25 seconds. This allows visualization of the first regions that achieve maximal stress and strains tensors (Fig. 15). After analysis of the results, under the same conditions the load transmission capacity in the osteoporotic bone was reduced up to approx. 23% compared with the healthy biopsy after interpreting von Mises stress and minimum principal strain distribution. It appears that the size of osteocytes is more important than their number. Of course these findings need to be confirmed by analyzing more bone samples not only for the same region but other anatomical regions from healthy subjects and osteoporotic patients.

Fig. 14. Detail (through-view) of the FE-Mesh of the bone and osteocytes embedded in the bone matrix.
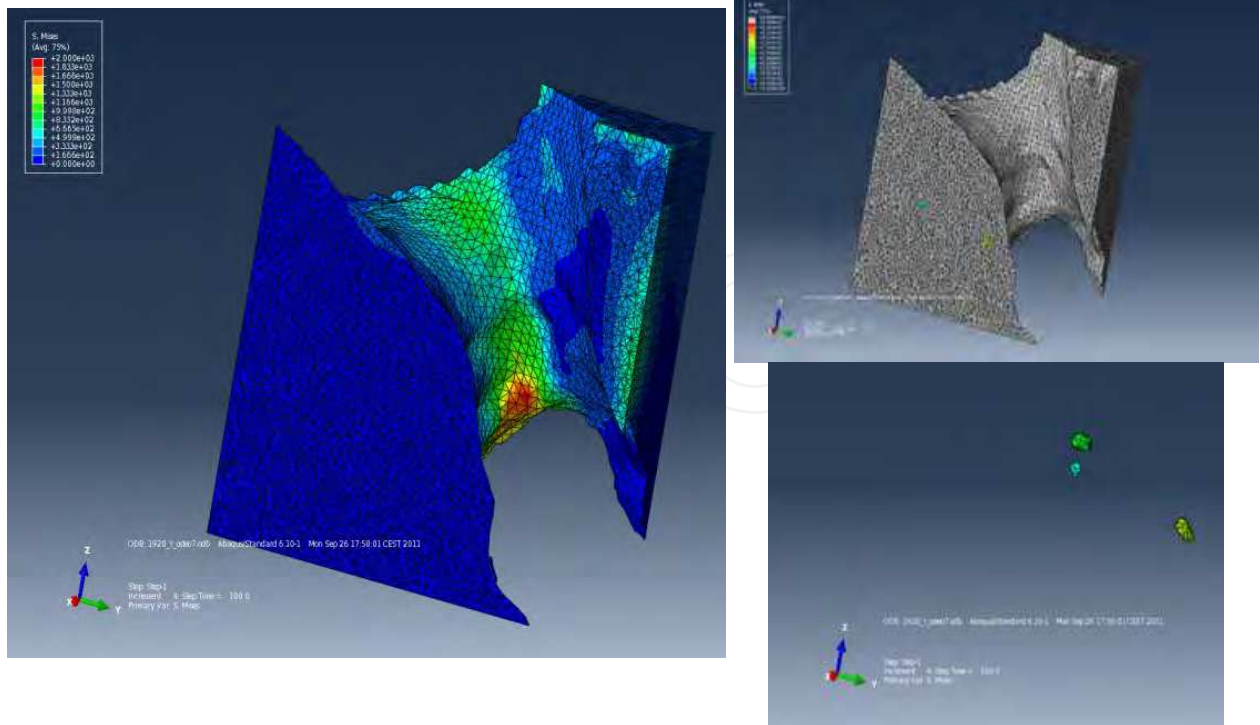

Fig. 15. von Mises stress distribution for a bone section and selected osteocytes with high stress values.

5. Specific scientific relevance and innovative aspects of osteocytes characterization

CT-Techniques and image analysis already allow bone structure, geometry and density evaluation over time (*in vivo*) or its detailed analysis at the nanometer scale (*in vitro*). However, it appears to be more challenging to describe how bones respond to pharmacological treatment or new mechanical conditions. Considering that osteocytes are not only directly responsible for starting bone remodeling regions, but that their number, size and distribution in comparable bone volumes shows how bone changed due to diseases or medications (e.g. as strontium ranelate or bisphosphonates, which alter bone mineralization), we have therefore developed a methodology for osteocytes characterization. For the first time, the complete method from laboratory CT (using a standard resolution of 20 μm), SR-CT (voxel size 2.174 μm) up to their finite element analysis was carried out.

Considering the actual developments in software and hardware, it has become possible not only to measure and reconstruct the bone biopsies using both 20 μm (laboratory CT) but also for the first time the total volume biopsy (2.2 mm diameter and 1cm length) using 2.174 μm isotropic resolution. It was important to visualize osteocytes distribution in their whole length and to verify the positioning of the osteocytes inside the total bone volume of the biopsy. The evaluation of bone biopsies (e.g. intact vs. unhealthy such as shown in this chapter, or after pharmacological treatments) will be a relevant and in the future important indicator for bone quality evaluation.

6. Potential users of the methodology and results

Once the relation between osteocytes and bone healthiness is understood, the methods described in this chapter will be used for the design of technologies to intervene in the mechanobiological process directed for the osteocytes. Patient specific pharmacological interventions or training conditions will be designed for it.

The method described here uses commercially available computational software and hardware and can easily be reproduced for visualization of the osteocytes lacunae and their processes distribution (to visualize this last a higher SR-CT resolution will be needed). In general, healthy bone matrix or its alterations due to genetics, aging or reduction in the bone mechanical stimuli could be studied and analyzed using this method.

In the future, the analysis of environment conditions and necessities of each patient will be carried out. After SR-CT measurements, its analysis requires advanced computational tools. Although the method described here is easy and reliable, it will not be readily available for all interested parties. Biopsies are an invasive technique. Maybe in the future and due to the continuous development in CTs technologies, reduced volume of bone samples will be sufficient for analysis but conserving the requirements of sufficient bone mass with a considerable number of osteocytes that allows comparisons and understanding bone diseases or bone response after usage of designed pharmacological interventions. However it remains speculative to suppose a minimal bone volume size to understand how osteocytes are acting. For future studies, it could be interesting for better understanding of osteocytes'

morphology and their role on bone behavior to analyze bone samples from regions with high turn-over metabolic process, thus to analyze osteocytes morphology and their interconnectivity. We propose the methodology described here as standard method, hence comparison between results from different studies will provide valuable knowledge on osteocytes nature.

7. Discussion

7.1 On the method

Considering that non necrotic bone tissue was present in the biopsies, it is assumed that in each osteocyte lacunae resides a living, active osteocyte with identical and normal functionality. Thus, the comparison of osteocytes morphology from bone samples, as e.g. osteoporotic and healthy analyzed and reported here, are valid providing information about relations between bone mechanics response and osteocytes morphology.

An obvious requirement is the measurement quality. For laboratory CT measurements, it is not critical because after reconstruction, it is possible to repeat the measurement in an adequate time. But, at least for the synchrotron measurements at BESSY, it was critical to repeat a SR-CT measurement, due to considerable time requirements for measuring and projections reconstruction and an inflexible time schedule. Thus, the selection of the biopsies and their preparations are not trivial at all.

One of the principal advantages of CT is its non-destructive nature, implying that measurements not only at different CT resolutions of the same samples and regions are possible, but it can also be combined with other techniques (e.g. atomic force microscope for studying the interaction with proteins). After comparisons of measured parameters at different scales, quantitative relations between density, bone structural parameters and number of osteocytes can be derived.

Combined CT techniques for measurement and reconstruction, image analysis and the finite element method are adequate to study and analyze osteocytes morphology and their relation with bone stiffness.

7.2 On the findings

As confirmed in this study the relation BV/TV is a good indicator of the bone quality. Considering that as observed in the laboratory μCT measurements (20 healthy and 20 osteoporotic bone biopsies) and observed in detail in the SR-CT measurements, in most cases the highest mineralized regions are localized at the center of each geometrical bone structure. Thus the possible effects on the ratios determination due to partial volume effects are counterbalanced independently from the scale used for scanning (of course for 20 μm and less).

After analysis of the first two biopsies selected for SR-CT measurements, the number of osteocytes for the healthy bone biopsy was clearly larger than for the osteoporotic bone sample, as expected, and although a major number of biopsies need to be analyzed this finding was confirmed after measurements of two additional samples. But an interesting fact was that osteocytes size appears to be smaller in the healthy bone biopsies.

8. Conclusion and future direction

Our findings showed a clear alignment of the osteocytes along the cement lines. Interestingly at the regions near the bone surface with reduced mineralization grade osteocytes were mainly aligned along the close to high mineralized region. Apparently, not only osteocytes number is reduced with aging but their size increases and become sparely distributed in comparison with the healthy bone samples from the human mandible.

Automatic tetrahedron mesh generation using the "tetragen" tool from Amira worked adequately for meshing the biopsies with a resolution of 20 µm, but meshing biopsies with osteocytes embedded on the bone matrix from the SR-CT samples consumes an enormous amount of time, due to necessary adjustments for avoiding intersections and conserving model closeness.

It is important to consider that this study has been initiated in 2008 (first scans with 20 µm) and remains an on-going study for performing the rest of SR-CT measurements, and for quantifying osteocytes/grade of mineralization. It was given importance to visualize osteocytes (lacunae) in the complete bone volume biopsy, and although the method has been established, new questions occurred: How is the grade of connectivity between osteocytes? Are there changes in the number and direction of the osteocytes dendrites for the osteoporotic and healthy bone biopsies? Is it possible that osteocytes for the osteoporotic bone samples are large but that all osteocytes possesses more or less the same number of processes (canaliculi), such that the number of canaliculi will become an specific characteristic of this bone cells? Or will due to aging a general mal-functioning of the osteocytes occur, such that only a reduced number of processes will be expected? In this last case, the pathway of the mechanical stimuli to osteoblastic and osteoclastic bone cell will be interrupted, and bone formation will never be initiated for regions with unconnected osteocytes and new bone will not be formed, similarly bone resorption required for initiating bone repair will be stopped.

8.1 Future direction

To finalize with such speculations, new measurements of the same 4 biopsies measured at BESSY with 2.174 µm (results report in this chapter) have been performed using a resolution of approx. 0.2 µm. We expect to see the canaliculi network, to perform 3D volume visualization and their quantitative analysis, following the established protocol presented here.

Additionally and since in osteoporotic bones osteocytes size appears to be larger as for healthy, additional analysis on the sample group included in this study will be performed for confirming or neglecting this finding. If the initial finding is true, it could be important to analyze if the grade of mineralization and number, size and distribution of osteocytes are related. SR-CT is able to show different degrees of mineralization. These analyses will be then realized at short time by including additional steps using the skeletonization tool after segmentation of the different mineralized regions in Amira, allowing their quantification and comparison.

There are some reports about the morphology and connectivity between osteocytes. However it is not clear how they are distributed in relation to the different grades of

mineralization. The SR-CT measurements using 0.2 μm spatial resolution will clarify this point.

Although not shown in this chapter, as the analysis has not been completed, we observe some micro- fissures whose pattern extended in 3D through complete biopsy, which we will be analyzed.

Visualization of osteocytes in their natural environment facilitates interpretation of the findings. Thus one can understand their role in the bone architecture by means of their morphological characterization.

9. Acknowledgments

10. References

Anderson, C. T., Castillo, A. B., Brugmann, S. A., Helms, J. A., Jacobs, C. R. and Stearns, T. Primary cilia: cellular sensors for the skeleton. *Anat Rec (Hoboken)* Vol.291,(9), 2008, pp:1074-8.

Beraudi, A., Stea, S., Bordini, B., Baleani, M. and Viceconti, M. Osteon classification in human fibular shaft by circularly polarized light. *Cells Tissues Organs* Vol.191,(3), 2010, pp:260-8.

Boutroy, S., Van Rietbergen, B., Sornay-Rendu, E., Munoz, F., Bouxsein, M. L. and Delmas, P. D. Finite element analysis based on in vivo HR-pQCT images of the distal radius is associated with wrist fracture in postmenopausal women. *J Bone Miner Res* Vol.23,(3), 2008, pp:392-9.

Boyde, A., Travers, R., Glorieux, F. H. and Jones, S. J. The mineralization density of iliac crest bone from children with osteogenesis imperfecta. *Calcif Tissue Int* Vol.64,(3), 1999, pp:185-90.

Cheung, W. Y., Liu, C., Tonelli-Zasarsky, R. M., Simmons, C. A. and You, L. Osteocyte apoptosis is mechanically regulated and induces angiogenesis in vitro. *J Orthop Res* Vol.29,(4), 2011, pp:523-30.

Cooper, D. M., Erickson, B., Peele, A. G., Hannah, K., Thomas, C. D. and Clement, J. G. Visualization of 3D osteon morphology by synchrotron radiation micro-CT. *J Anat*, 2011.

Cowin, S. C. Mechanosensation and fluid transport in living bone. *J Musculoskelet Neuronal Interact* Vol.2,(3), 2002, pp:256-60.

Dong, X. N., Zoghi, M., Ran, Q. and Wang, X. Collagen mutation causes changes of the microdamage morphology in bone of an OI mouse model. *Bone* Vol.47,(6), 2010, pp:1071-5.

Feng, J. Q., Ward, L. M., Liu, S., Lu, Y., Xie, Y., Yuan, B., Yu, X., Rauch, F., Davis, S. I., Zhang, S., Rios, H., Drezner, M. K., Quarles, L. D., Bonewald, L. F. and White, K. E. Loss of DMP1 causes rickets and osteomalacia and identifies a role for osteocytes in mineral metabolism. *Nat Genet* Vol.38,(11), 2006, pp:1310-5.

Fouard, C., Malandain, G., Prohaska, S. and Westerhoff, M. Blockwise processing applied to brain microvascular network study. *IEEE Trans Med Imaging* Vol.25,(10), 2006, pp:1319-28.

Han, Y., Cowin, S. C., Schaffler, M. B. and Weinbaum, S. Mechanotransduction and strain amplification in osteocyte cell processes. *Proc Natl Acad Sci U S A* Vol.101,(47), 2004, pp:16689-94.

Huang, C. and Ogawa, R. Mechanotransduction in bone repair and regeneration. *Faseb J* Vol.24,(10), 2010, pp:3625-32.

Huiskes, R. If bone is the answer, then what is the question? *J Anat* Vol.197,(Pt 2), 2000, pp:145-156.

Jacobs, C. R., Temiyasathit, S. and Castillo, A. B. Osteocyte mechanobiology and pericellular mechanics. *Annu Rev Biomed Eng* Vol.12, 2010, pp:369-400.

Kearney, E. M., Farrell, E., Prendergast, P. J. and Campbell, V. A. Tensile strain as a regulator of mesenchymal stem cell osteogenesis. *Ann Biomed Eng* Vol.38,(5), 2010, pp:1767-79.

Kerschnitzki, M., Wagermaier, W., Roschger, P., Seto, J., Shahar, R., Duda, G. N., Mundlos, S. and Fratzl, P. The organization of the osteocyte network mirrors the extracellular matrix orientation in bone. *J Struct Biol* Vol.173,(2), 2011, pp:303-11.

Liu, X. Y. Effects of microgravity on Ca mineral crystallization and implication for osteoporosis in space. *Applied Physics Letters* Vol.79,(21), 2001, pp:3539-41.

Mulvihill, B. M. and Prendergast, P. J. An algorithm for bone mechanoresponsiveness: implementation to study the effect of patient-specific cell mechanosensitivity on trabecular bone loss. *Comput Methods Biomech Biomed Engin* Vol.11,(5), 2008, pp:443-51.

Nabavi, N., Khandani, A., Camirand, A. and Harrison, R. E. Effects of microgravity on osteoclast bone resorption and osteoblast cytoskeletal organization and adhesion. *Bone*, 2001.

Perilli, E., Baruffaldi, F., Visentin, M., Bordini, B., Traina, F., Cappello, A. and Viceconti, M. MicroCT examination of human bone specimens: effects of polymethylmethacrylate embedding on structural parameters. *J Microsc.* Vol.225,(Pt 2), 2007, pp:192-200.

Rack, A., Zabler, S., Mueller, B. R., Riesemeier, H., Weidemann, G., Lange, A., Goebbels, J., Hentschel, M. and Goerner, W. High resolution synchrotron-based radiography and tomography using hard X-rays at the BAMline (BESSY II). *Nuclear Instruments and Methods in Physics Research Section A* Vol.586,(2), 2008, pp:327-344.

Rincon-Kohli, L. and Zysset, P. K. Multi-axial mechanical properties of human trabecular bone. *Biomech Model Mechanobiol* Vol.8,(3), 2009, pp:195-208.

Rodionova, N. V., Oganov, V. S. and Zolotova, N. V. Ultrastructural changes in osteocytes in microgravity conditions. *Adv Space Res* Vol.30,(4), 2002, pp:765-70.

Roschger, P., Paschalis, E. P., Fratzl, P. and Klaushofer, K. Bone mineralization density distribution in health and disease. *Bone* Vol.42,(3), 2008, pp:456-66.

Schneider, P., Meier, M., Wepf, R. and Muller, R. Serial FIB/SEM imaging for quantitative 3D assessment of the osteocyte lacuno-canalicular network. *Bone* Vol.49,(2), 2011, pp:304-11.

Stalling, D., Westerhoff, M., and Hege, H.-C. (2005). Amira: a highly interactive system for visual data analysis. *The Visualization Handbook*. C. D. Hansen, and Johnson, Christopher R., Elsevier: 749-767.

van Oers, R. F., Ruimerman, R., van Rietbergen, B., Hilbers, P. A. and Huiskes, R. Relating osteon diameter to strain. *Bone* Vol.43,(3), 2008, pp:476-82.

Varga, P., Pahr, D. H., Baumbach, S. and Zysset, P. K. HR-pQCT based FE analysis of the most distal radius section provides an improved prediction of Colles' fracture load in vitro. *Bone* Vol.47,(5), 2011, pp:982-8.

Vilayphiou, N., Boutroy, S., Szulc, P., Van Rietbergen, B., Munoz, F., Delmas, P. D. and Chapurlat, R. Finite element analysis performed on radius and tibia HR-pQCT images and fragility fractures at all sites in men. *J Bone Miner Res*, 2011.

Whitfield, J. F. Primary cilium--is it an osteocyte's strain-sensing flowmeter? *J Cell Biochem* Vol.89,(2), 2003, pp:233-7.

You, L., Cowin, S. C., Schaffler, M. B. and Weinbaum, S. A model for strain amplification in the actin cytoskeleton of osteocytes due to fluid drag on pericellular matrix. *J Biomech* Vol.34,(11), 2001, pp:1375-86.
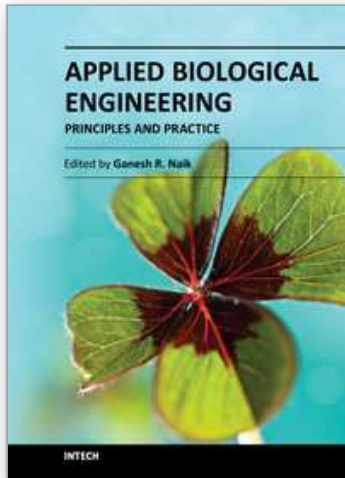
Applied Biological Engineering - Principles and Practice

Edited by Dr. Ganesh R. Naik

Biological engineering is a field of engineering in which the emphasis is on life and life-sustaining systems. Biological engineering is an emerging discipline that encompasses engineering theory and practice connected to and derived from the science of biology. The most important trend in biological engineering is the dynamic range of scales at which biotechnology is now able to integrate with biological processes. An explosion in micro/nanoscale technology is allowing the manufacture of nanoparticles for drug delivery into cells, miniaturized implantable microsensors for medical diagnostics, and micro-engineered robots for on-board tissue repairs. This book aims to provide an updated overview of the recent developments in biological engineering from diverse aspects and various applications in clinical and experimental research.

How to reference

In order to correctly reference this scholarly work, feel free to copy and paste the following:

Zully Ritter, Andreas Staude, Steffen Prohaska and Dieter Felsenberg (2012). Osteocytes Characterization Using Synchrotron Radiation CT and Finite Element Analysis, Applied Biological Engineering - Principles and Practice, Dr. Ganesh R. Naik (Ed.), ISBN: 978-953-51-0412-4, InTech, Available from: http://www.intechopen.com/books/applied-biological-engineering-principles-and-practice/osteocytes-characterization-using-synchrotron-radiation-ct-and-finite-element-analysis

INTECH
open science | open minds